Poly(ether imide)s from Diamines with *Para*-, *Meta*-, and *Ortho*-Arylene Substitutions: Synthesis, Characterization, and Liquid Crystalline Properties

Theo J. Dingemans,*,† Eduardo Mendes,‡ Jeffrey J. Hinkley,§ Erik S. Weiser,§ and Terry L. StClair§

Faculty of Aerospace Engineering, Delft University of Technology, Kluyverweg 1, 2629 HS Delft, The Netherlands; Section Nanostructured Materials, Delft University of Technology, Julianalaan 136, 2628 BL, Delft, The Netherlands; and Advanced Materials and Processing Branch, NASA Langley Research Center; Hampton, Virginia 23681-2199

Received January 6, 2008; Revised Manuscript Received February 2, 2008

ABSTRACT: We have synthesized homologous series of *para*-, *meta*-, and *ortho*-substituted aryl ether diamine monomers, with either 2, 3, or 4 ether linkages per monomer unit, and prepared their corresponding poly(ether imide)s with 3,3′,4,4′-biphenyl dianhydride (BPDA) and 3,3′,4,4′-oxydiphthalic dianhydride (ODPA). All polymers were obtained in high molecular weights and gave good quality films with expected mechanical and thermal properties. The *ortho*- and *meta*-substituted diamines gave fully amorphous polymers, whereas the *para*-based diamines resulted in semicrystalline polymers. The glass-transition temperatures (T_g) drop in the order of *para* > *ortho* > *meta*, and the T_g drops considerably as a function of the aryl ether content and appears to level off at four ether linkages. The T_g values of our polymers were contrasted with a simple quantitative model and found to be in good agreement with the experimental results (±10 °C). BPDA in combination with an all *para*-substituted, aryl ether-based diamine (BPDA-***P3***) forms a thermotropic liquid crystalline phase. Optical microscopy experiments confirm the presence of a nematic melt. Highly aligned films could easily be obtained by stretching the films in the liquid crystal phase, and XRD analysis of quenched films confirmed the presence of a highly aligned smectic A phase (SmA) with an order parameter $\langle P_2 \rangle = 0.87$, indicating a high degree of molecular alignment. To the best of our knowledge, this is the first example of an all-aromatic liquid crystalline poly(ether imide). Dynamic mechanical thermal analysis (DMTA) showed that the *para*-aryl ethers display broad β-transitions (25–160 °C), whereas the *meta*- and *ortho*-series do not show β-transitions. All PEIs with 3 or 4 aryl ether linkages become thermoplastic in nature. The purpose of this systematic study is to provided a basic set of design rules toward the design and synthesis of all-aromatic poly(ether imide) architectures.

1. Introduction

All-aromatic poly(ether imide)s (PEIs) are high-performance polymers which are well-known for their excellent thermal, mechanical, and electric properties.[1] However, all-aromatic PEIs are difficult to melt process because they exhibit high softening temperatures (T_g) and melting temperatures (T_m). The processability can be improved by introducing flexible groups such as aliphatic moieties, but this will significantly reduce the thermal stability of these polymers. A more successful approach to improving the processability is to design all-aromatic ether−imide-based oligomers, end-capped with reactive functionalities such as phenylethynyl.[2] The polymer molecular weight is reduced, which will improve the processability, and the thermal and mechanical properties are outstanding after cure. Another route would be to design an all-aromatic liquid crystalline poly(ether imide). The improved melt processability, the low coefficient of thermal expansion (CTE), and barrier properties associated with the mesophase combined with the thermal stability of aromatic ether imides would provide a new family of materials useful for aeronautic and space applications as well as for electronics and other demanding applications. Several researchers have shown that liquid crystalline polyimides are indeed possible when aliphatic spacers or ester functionalities were employed to lower the melting temperatures. Doing so compromised the thermal stability of the resulting polymers, however.[3] In order to circumvent these problems, an all-aromatic ether−imide-based backbone architecture is required. To date, no wholly aromatic liquid crystalline poly(ether imide)s have been reported.

Recently, we published our results on a series of wholly aromatic ether−imide model compounds[4] of the "tail−core−tail" type. Different dianhydrides were used as the rigid core moiety, i.e., pyromellitic dianhydride (PMDA), 1,4,5,8-naphthalenetetracarboxylic dianhydride (NDA), 3,3′,4,4′-biphenyltetracarboxylic dianhydride (BPDA), and 3,3′,4,4′-oxydiphthalic dianhydride (ODPA), and they were terminated with *meta*-substituted aromatic ether−amine flexible tails. Although the model compounds fit the classic description of mesogenic compounds, we could only detect mesomorphism in one model compound, i.e., **NDA-n$_0$**. This compound exhibits a monotropic smectic A (S_A) and columnar phase (Col) on cooling.

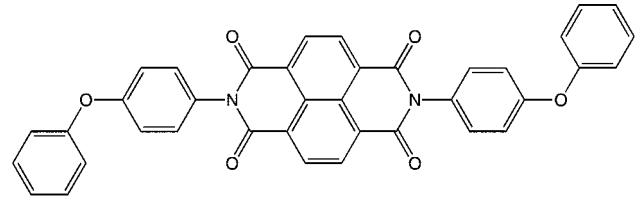

NDA-n$_0$; K - 310.3 - D_{rd} - 333.3 - S_A - 335.0 - I

In an attempt to fully understand the structure–property relationships in all-aromatic poly(ether imide)s and determine which factors lead to mesophase formation, we synthesized three series of aryloxy-based diamines. The diamines were designed

* To whom correspondence should be addressed. E-mail: t.j.dingemans@tudelft.nl.
† Faculty of Aerospace Engineering, Delft University of Technology.
‡ Section Nanostructured Materials, Delft University of Technology.
§ NASA Langley Research Center.

10.1021/ma8000324 CCC: $40.75
Published on Web 03/15/2008

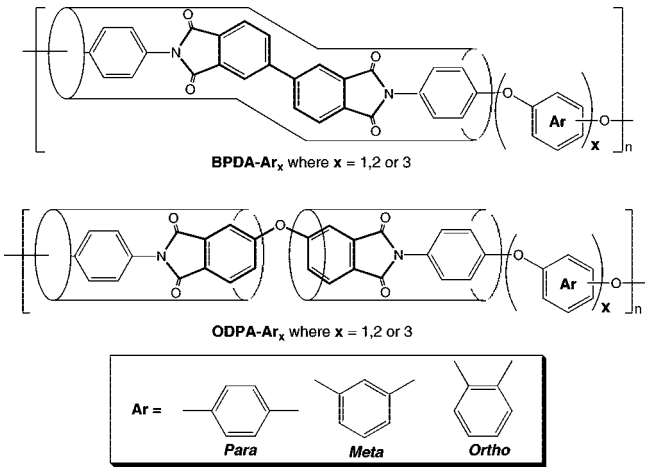

Figure 1. Structures of the main-chain poly(ether imide)s with *para*, *meta*-, or *ortho*-based aryl ether "flexible" spacers.

so that the terminal phenylamine functionality would increase the aspect ratio of the selected rigid diimide core, while the *para*-, *meta*-, or *ortho*-substituted aryl ether units would provide flexibility and lower the melting point of the resulting polymer. The diamines were reacted with 3,3′,4,4′-biphenyltetracarboxylic dianhydride (BPDA) and 3,3′,4,4′-oxydiphthalic dianhydride (ODPA). The polymers are shown in Figure 1, where the rigid cores are accentuated.

2. Experimental Section[5]

2.1. Characterization. The structures of the final products were confirmed using ^{1}H NMR and ^{13}C NMR spectroscopy. The spectra were recorded using a Bruker Avance 300 spectrometer (300 MHz). Infrared spectra were collected using a Nicolet Magna-IR Spectrometer 750, and mass spectra (MS) were obtained with a Hewlett-Packard 5972 spectrometer, with M+ representing the molecular ion.

Transition temperatures were determined using a Perkin-Elmer Pyris differential scanning calorimeter (DSC), calibrated with indium (99.99%) (mp 156.5 °C, $\Delta H = 28.315$ J/g) and tin (99.99%) (mp 232.0 °C, $\Delta H = 54.824$ J/g). Heating and cooling scans were recorded at 10 °C/min. Thermogravimetric studies (TGA) were conducted with a Seiko TGA-220 under nitrogen or air atmosphere using a heating rate of 2.5 °C/min after a 1 h hold at 100 °C. Melting points of intermediates and monomers were determined with a Electrothermal digital melting point apparatus IA 9000 series using a heating rate of 2.5 °C/min. The melt behavior of the polymer films was studied using an Olympus BH-2 optical microscope, equipped with a Mettler Toledo FP82H hot stage. Samples were examined between glass microscope slides.

Polymer thin films were investigated using a Rheometric Scientific dynamic mechanical thermal analyzer, DMTA-IV, operated at a heating rate of 2.5 °C/min from 30 to 400 °C, at 1 Hz under a nitrogen atmosphere.

2.2. Materials. All common start materials and reagents were obtained from Aldrich Chemical Co. 3,3′,4,4′-Biphenyltetracarboxylic dianhydride (BPDA) and 1,4-bis(4-aminophenoxy)benzene (***P*1**) were purchased from Chriskev Co. Inc. 3,3′,4,4′-Oxydiphthalic dianhydride (OPDA) was purchased from Occidental Chemical Corp., and 1,3-bis(4-aminophenoxy)benzene (***M*1**) and 1,3-bis(3-aminophenoxy)benzene were available from Mitsui Toatsu Chemicals Inc. *N*-Methyl-2-pyrrolidinone (NMP), *N,N*-dimethylacetamide (DMAc), toluene, and pyridine were dried over, and distilled from, CaH_2 prior to use. All other materials were used as received.

2.3. Monomer Synthesis. *Bis[4-(4-nitrophenoxy)phenyl] Ether (**2**).* A 250 mL two-neck flask equipped with an overhead stirrer, nitrogen inlet, and a Dean–Stark trap with reflux condenser was charged with 4.65 g (0.023 mol) of 4,4′-oxydiphenol (**1**), 6.99 g (0.051 mol) of finely ground K_2CO_3, 80 mL of DMAc, and 80 mL of toluene. This mixture was stirred and heated at 135 °C for 1.5 h, after which the temperature was increased to 175 °C. The theoretical amount of water was collected in the Dean–Stark trap and removed together with the toluene. The dark reaction mixture was cooled to room temperature, and 8.11 g (0.058 mol) of 1-fluoro-4-nitrobenzene was added, and this mixture was heated to 160 °C overnight. After the reaction mixture was cooled to room temperature, 200 mL of water was slowly added. This mixture was extracted with 200 mL of CH_2Cl_2 (3×), and the organic layer was washed with 200 mL of water (2×) and dried over $MgSO_4$. After removing the solvent, the crude product was recrystallized from acetone/ethanol (50/50). Bis[4-(4-nitrophenoxy)phenyl] ether (**2**) was obtained as bright yellow crystals. Yield: 9.5 g (93%); TLC (9/1 hexane/ethyl acetate) $t_r = 0.5$ (one spot); mp: 137–138 °C (136 °C).[6]

*Bis[4-(4-aminophenoxy)phenyl] Ether (**P2**).* A 150 mL hydrogenation bottle was charged with 9.5 g (0.021 mol) of bis[4-(4-nitrophenoxy)phenyl] ether, 100 mL of dry THF, and 0.9 g of 10% Pd−C. The bottle was placed in a Parr hydrogenator, and the nitro group was reduced under H_2 atmosphere (50 psi) for 5 h at room temperature. The THF solution was filtered over a short silica gel/celite patch, and the THF was removed by distillation. Pure bis[4-(4-aminophenoxy)phenyl] ether (***P*2**) was obtained after recrystallization from ethanol as beige crystals. Yield: 7.8 g (95%); TLC (CH_2Cl_2) $t_r = 0.05$ (one spot); mp: 108 °C (109 °C).[6] IR(KBr): υ_{max} 3384, 3316, 1502, 1276, 1225, 1191, 1105, 1099, 868, 844, 830, 805 cm^{-1}. ^{1}H NMR ($CDCl_3$) δ (ppm): 3.55 (s, 4H), 6.64 (d, 4H, $J = 10$ Hz), 6.83 (d, 4H, $J = 10$ Hz), 6.88 (s, 8H). ^{13}C NMR ($CDCl_3$) δ (ppm): 116.1, 118.6, 119.5, 120.4, 142.4, 149.1, 152.4, 154.1.

*4-Aryloxydialdehyde (**4**).* A 500 mL two-neck flask equipped with a magnetic stirrer, reflux condenser, and nitrogen inlet was charged with 11.01 g (0.1 mol) of hydroquinone (**3**), 27.6 g (0.2 mol) of finely ground K_2CO_3, and 250 mL of DMAc. This mixture was stirred and refluxed for 5 h. The dark reaction mixture was cooled to room temperature and diluted with water, and the beige product was collected, washed with water, and dried. The crude product was recrystallized from isopropanol/DMAc (90/10). The 4-aryloxydialdehyde (**4**) was obtained as beige crystals. Yield: 23 g (72%); TLC (9/1 hexane/ethyl acetate) $t_r = 0.38$ (one spot); mp: 158–159 °C (158 °C).[7]

*1,4-Bis(4-hydroxyphenoxy)benzene (**5**).* To a stirred solution of 12.7 g (0.04 mol) of 4-aryloxydialdehyde (**4**) in 100 mL of $CHCl_3$ was added 21.5 g (0.1 mol) of *m*-CPBA. The reaction mixture was stirred for 2 h at room temperature. The solution was washed with $NaHSO_3$ (100 mL), $NaHCO_3$ (2 × 100 mL), and water (100 mL). The solvent was removed by distillation, and the crude product was recrystallized from methanol/water (95/5). Yield: 11.1 g (79%). The 4-aryloxy bisformate intermediate (7 g, 0.02 mol) was dissolved in 100 mL of methanol and treated with a 0.5 M KOH/methanol solution (10 mL). The reaction mixture was heated to refluxed for 1 h. The solvent was removed by distillation, and the crude product was treated with a 1 M HCl solution. The crude product was collected by filtration, dried, and recrystallized from toluene/isopropanol (90/10). 1,4-Bis(4-hydroxyphenoxy)benzene (**5**) was obtained as off-white crystals. Yield: 5 g (85%). TLC (9/1 hexane/ethyl acetate) $t_r = 0.1$ (one spot); mp: 187–189 °C (187 °C).[7]

*1,4-Bis[4-(4-nitrophenoxy)phenoxy]benzene (**6**).* Its synthetic procedure is similar to that of bis[4-(4-nitrophenoxy)phenyl] ether (**2**). Off-white crystals. Yield: 7.9 g (74%). TLC (9/1 hexane/ethyl acetate) $t_r = 0.5$ (one spot); mp: 142–143 °C. ^{1}H NMR ($CDCl_3$) δ (ppm): 6.99 (d, 4H, $J = 9$ Hz), 7.04 (s, 4H), 7.05 (s, 8H), 8.18 (d, 4H, $J = 9$ Hz). ^{13}C NMR ($CDCl_3$) δ (ppm): 116.7, 119.9, 120.6, 122, 122.1, 126, 149.9, 152.9, 155.1, 163.8.

*1,4-Bis[4-(4-aminophenoxy)phenoxy]benzene (**P3**).* Its synthetic procedure is similar to that of bis[4-(4-aminophenoxy)phenyl] ether (***P*2**). Off-white crystals after recrystallization from acetone/water (95/5). Yield: 6.2 g (86%); mp: 170 °C. IR (KBr): υ_{max} 3384, 3316, 1499, 1275, 1223, 1193, 1105, 1097, 865, 846, 827 cm^{-1}. ^{1}H NMR ($CDCl_3$) δ (ppm): 3.55 (s, 4H), 6.64 (d, 4H, $J = 9$ Hz), 6.83 (d, 4H, $J = 9$ Hz),

6.87–6.93 (m, 12H). ^{13}C NMR ($CDCl_3$) δ (ppm): 116.2, 118.6, 119.5, 119.7, 119.8, 120.5, 142.4, 149.1, 152.2, 153.1, 154.3.

*Bis(3-methoxyphenyl) Ether (**8**).* A 500 mL two-neck flask equipped with a stir bar, a nitrogen inlet, and distillation apparatus was charged with 9.46 g (0.175 mol) of sodium methoxide and 200 mL of dry toluene. Using an addition funnel, 16.76 g (0.09 mol) of 3-methoxyphenol (**7**) was slowly added, and after the reaction was completed, the reaction mixture was heated and methanol and toluene were distilled off, leaving a white phenoxy salt. The salt was cooled to room temperature, and a reflux condenser was fitted on the flask and 200 mL of dry pyridine was added. This solution was heated to reflux and in a stream of nitrogen; 67.3 g (0.36 mol) of 3-bromoanisole was added all at once, followed immediately by 2.7 g (0.027 mol) of CuCl. This reaction mixture was stirred at reflux for 12 h under a nitrogen atmosphere and cooled to room temperature. The reaction mixture was quenched with 300 mL of 18% HCl and extracted with 100 mL of diethyl ether (3×). The organic layer was washed with 250 mL of water and dried over $MgSO_4$. The dry ether solution was filtered over a short patch of silica gel/celite in order to remove the copper salts. The solvent and excess 3-methoxyphenol were removed by vacuum distillation, and the bis(3-methoxyphenyl) ether (**8**) was obtained at as a pale yellow oil at 95 °C/500 mTorr. Yield: 24.7 g (60%). TLC (9/1 hexane/ethyl acetate) $t_r = 0.6$ (one spot); MS (*m*/*z*): 230 (M+), 215, 199, 187, 171, 159, 144, 128.

*3,3′-Oxydiphenol (**9**).* A 200 mL one-neck flask equipped with stir bar and reflux condenser was charged with 11.5 g (0.05 mol) of bis(3-methoxyphenyl) ether (**8**), 160 mL of glacial acetic acid, and 115 mL of HBr (48%). This solution was refluxed for 5 h and allowed to cool to room temperature. The orange solution was extracted with 200 mL of CH_2Cl_2, and the organic layer was washed with 150 mL of water (2×) and dried over $MgSO_4$. The solvent was removed, and the 3,3′-oxydiphenol (**9**) was used for the next step without further purification. Yield: 6.1 g (60%); mp: 94–95 °C (94–96 °C).[8] TLC (9/1 hexane/ethyl acetate) $t_r = 0.1$ (one spot).

*Bis[3-(4-nitrophenoxy)phenyl] Ether (**10**).* Its synthetic procedure is similar to that of bis[4-(4-nitrophenoxy)phenyl] ether (**2**). Bright yellow powder. Yield: 8.7 g (65%); TLC (9/1 hexane/ethyl acetate) $t_r = 0.5$ (one spot); MS (*m*/*z*): 444 (M+), 278, 168, 139, 128.

*Bis[3-(4-aminophenoxy)phenyl] Ether (**M2**).* Its synthetic procedure is similar to that of bis[4-(4-aminophenoxy)phenyl] ether (***P2***). Slow crystallizing yellow oil. Yield: 7.3 g (90%); mp: 73–75 °C. TLC (9/1 hexane/ethyl acetate) $t_r = 0.05$ (one spot). IR (KBr): υ_{max} 3405, 3323, 3220, 1621, 1589, 1506, 1476, 1274, 1207, 1138, 1122, 985, 963, 846, 759 cm^{-1}. ^{1}H NMR ($CDCl_3$) δ (ppm): 3.45 (s, 2H), 6.59–6.67 (m, 5H), 6.85 (d, 2H, $J = 9$ Hz), 7.18 (t, 1H, $J = 8$ Hz). ^{13}C NMR ($CDCl_3$) δ (ppm): 108.0, 111.8, 112.2, 116.1, 121.2, 130.1, 142.9, 147.9, 157.9.

*1,3-Bis(3-hydroxyphenoxy)benzene (**12**).* A 200 mL beaker was charged with 11.7 g (0.04 mol) of 1,3-bis(3-aminophenoxy)benzene (**11**) and 50 mL of H_2SO_4 (35%) was slowly added. The solution was cooled to 10 °C, and 40 g of ice was added. A solution of 6.62 g (0.096 mol) of $NaNO_2$ in water (40 mL) was added at such a rate that the reaction temperature did not exceed 5 °C. The bright yellow diazonium solution was kept at 0 °C and slowly added to a boiling solution of H_2O/H_2SO_4 (200 mL/35%). After complete addition the dark red reaction mixture was cooled to room temperature and extracted with 200 mL of ethyl ether (3×). The organic layer was washed with 100 mL of water (3×) and dried over $MgSO_4$. After removing the ethyl ether by distillation, 1,3-bis(3-hydroxyphenoxy)benzene (**12**) was obtained as a dark red oil and was used for the next step without further purification.

*1,3-Bis[3-(4-nitrophenoxy)phenoxy]benzene (**13**).* Its synthetic procedure is similar to that of bis[4-(4-nitrophenoxy)phenyl] ether (**2**). Bright yellow crystals. Yield: 7.4 g (69%); TLC (9/1 hexane/ethyl acetate) $t_r = 0.45$ (one spot); mp: 58–60 °C. MS (*m*/*z*): 536 (M+), 260, 168, 139.

*1,3-Bis[3-(4-aminophenoxy)phenoxy]benzene (**M3**).* Its synthetic procedure is similar to that of bis[4-(4-aminophenoxy)phenyl]ether (***P2***). Slow crystallizing oil, recrystallized from (75/25 ethanol/water). Yield: 1.96 g (88%). TLC (9/1 hexane/ethyl acetate) $t_r = 0.1$ (one spot); mp: 38–40 °C. IR(KBr): υ_{max} 3406, 3369, 3221, 1590, 1507, 1476, 1263, 1208, 1136, 983, 835, 771 cm^{-1}. ^{1}H NMR ($CDCl_3$) δ (ppm): 3.42 (s, 2H), 6.59–6.65 (m, 11H), 6.70 (dd, 2H, $J = 9$ Hz), 6.85 (d, 4H, $J = 8$ Hz), 7.14–7.23 (m, 3H). ^{13}C NMR ($CDCl_3$) δ (ppm): 108.0, 109.4, 111.9, 112.3, 113.4, 116.1, 121.2, 130.1, 130.3, 142.9, 147.8, 157.7, 158.1, 160.1.

*1,2-Bis(4-nitrophenoxy)benzene (**15**).* Its synthetic procedure is similar to that of bis[4-(4-nitrophenoxy)phenyl] ether (**2**). Recrystallized from ethanol. Yield: 26.2 g (74%); mp: 135–136 °C (134–135 °C).[9] TLC (9/1 hexane/ethyl acetate) $t_r = 0.15$ (one spot).

*1,2-Bis(4-aminophenoxy)benzene (**O1**).* Its synthetic procedure is similar to that of bis[4-(4-aminophenoxy)phenyl] ether (***P2***). Recrystallized from ethanol. Yield: 14.2 g (86%); mp: 134–135 °C (135–136 °C).[9] IR (KBr): υ_{max} 3448, 3362, 3195, 1617, 1583, 1505, 1449, 1254, 1209, 1105, 888, 832, 765 cm^{-1}. TLC (9/1 hexane/ethyl acetate) $t_r = 0$ (one spot). ^{1}H NMR ($CDCl_3$) δ (ppm): 3.51 (s, 4H), 6.60 (d, 4H, $J = 9$ Hz), 6.81 (d, 4H, $J = 9$ Hz), 6.9–7.1 (m, 4H); ^{13}C NMR ($CDCl_3$) δ (ppm): 116, 119, 119.8, 123, 142, 148.5, 149.1.

Bis(2-methoxyphenyl) Ether. Its synthetic procedure is similar to that of bis(3-methoxyphenyl) ether (**8**). The solvent, unreacted guaiacol, and 2-bromoanisole were removed by vacuum distillation. Pure bis(2-methoxyphenyl)ether (**17**) was obtained after recrystallization from ethanol. Yield: 25.4 g (61%). TLC (9/1 hexane/ethyl acetate) $t_r = 0.3$ (one spot); mp: 76–78 °C (77–79 °C).[10] MS (*m*/*z*): 230 (M+), 184, 121.

*2,2′-Oxydiphenol (**18**).* Its synthetic procedure is similar to that of 3,3′-oxydiphenol (**9**). Recrystallized from hot water. Yield: 6.1 g (60%); mp: 123 °C (122–123 °C).[10] TLC (9/1 hexane/ethyl acetate) $t_r = 0.11$ (one spot).

*Bis[2-(4-nitrophenoxy)phenyl] Ether (**19**).* Its synthetic procedure is similar to that of bis[4-(4-nitrophenoxy)phenyl] ether (**2**). Recrystallized from ethanol. Yield: 10 g (98%); mp: 125–126 °C. TLC (9/1 hexane/ethyl acetate) $t_r = 0.18$ (one spot). ^{1}H NMR ($CDCl_3$) δ (ppm): 6.77 (d, 4H, $J = 9$ Hz), 7.01 (dd, 2H, $J = 8$ Hz), 7.10–7.25 (m, 6H), 8.04 (d, 4H, $J = 9$ Hz). ^{13}C NMR ($CDCl_3$) δ (ppm): 115.9, 120, 123.2, 125.1, 125.6, 126.8, 142.5, 144.2, 147.9, 162.7.

*Bis[2-(4-aminophenoxy)phenyl] Ether (**O2**).* Its synthetic procedure is similar to that of bis[4-(4-aminophenoxy)phenyl] ether (***P2***). Recrystallized from ethanol. Yield: 8.1 g (94%); mp: 152–154 °C. TLC (9/1 hexane/ethyl acetate) $t_r = 0.05$ (one spot). IR (KBr): υ_{max} 3458, 3370, 3210, 1625, 1507, 1452, 1267, 1244, 1201, 1110, 874, 844, 755 cm^{-1}. ^{1}H NMR ($CDCl_3$) δ (ppm): 3.49 (s, 4H), 6.54 (d, 4H, $J = 9$ Hz), 6.76 (d, 4H, $J = 9$ Hz), 6.85 (t, 2H, $J = 2$ Hz), 6.95 (s, 6H). ^{13}C NMR ($CDCl_3$) δ (ppm): 115.9, 118.9, 119.5, 120, 122.9, 123.7, 142, 147.2, 148.7, 148.9.

*1,2-Bis(2-methoxyphenoxy)benzene (**20**).* Its synthetic procedure is similar to that of bis(3-methoxyphenyl) ether (**8**). The solvent, excess start material, and monosubstituted side product were removed by vacuum distillation (Kugelrohr). The remaining red oil was diluted with hot acetone/hexane (95/5) and cooled to −20 °C. Pure 1,2-bis(2-methoxyphenoxy)benzene (**20**) was obtained as off-white crystals. Yield: 4.9 g (22%); T_m: 103–104 °C (102–104 °C).[11] TLC (9/1 hexane/ethyl acetate) $t_r = 0.18$ (one spot).

*1,2-Bis(2-hydroxyphenoxy)benzene (**21**).* Its synthetic procedure is similar to that of 3,3′-oxydiphenol (**9**). Yield: 6.1 g (95%); T_m: 91–93 °C (90–91 °C).[11] TLC (9/1 hexane/ethyl acetate) $t_r = 0.11$ (one spot).

*1,2-Bis[2-(4-nitrophenoxy)phenoxy]benzene (**22**).* Its synthetic procedure is similar to that of bis[4-(4-nitrophenoxy)phenyl]ether (**2**). Recrystallized from ethanol. Yield: 5.4 g (50%); T_m: 93–94 °C. TLC (9/1 hexane/ethyl acetate) $t_r = 0.17$ (one spot). ^{1}H NMR ($CDCl_3$) δ (ppm): 6.68 (dd, 2H, $J = 8$ Hz), 6.80 (d, 4H, $J = 9$ Hz), 6.85–6.95 (m, 2H), 6.97–7.17 (m, 8H), 8.00 (d, 4H, $J = 9$ Hz). ^{13}C NMR ($CDCl_3$) δ (ppm): 115.9, 118.3, 121.2, 123.1, 124, 125.3, 125.6, 126.7, 142.4, 143.4, 146.3, 148.9, 163.1.

*1,2-Bis[2-(4-aminophenoxy)phenoxy]benzene (**O3**).* Its synthetic procedure is similar to that of bis[4-(4-aminophenoxy)phenyl] ether (***P2***). Off-white crystals, recrystallized from ethanol. Yield: 4.1 g (82%); T_m: 135–136 °C. TLC (9/1 hexane/ethyl acetate) $t_r = 0.08$

Scheme 1. Synthesis of Bis[4-(4-aminophenoxy)phenyl] Ether (*P*2) and 1,4-Bis[4-(4-aminophenoxy)phenoxy]benzene (*P*3)

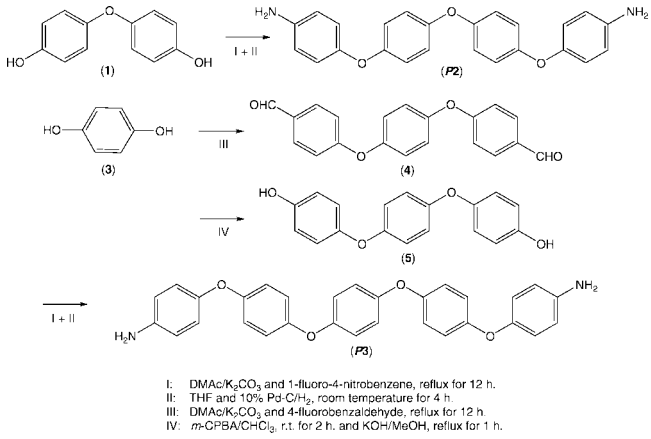

I: DMAc/K_2CO_3 and 1-fluoro-4-nitrobenzene, reflux for 12 h.
II: THF and 10% Pd-C/H_2, room temperature for 4 h.
III: DMAc/K_2CO_3 and 4-fluorobenzaldehyde, reflux for 12 h.
IV: *m*-CPBA/$CHCl_3$, r.t. for 2 h. and KOH/MeOH, reflux for 1 h.

(one spot). IR (KBr): υ_{max} 3472, 3442, 3383, 3364, 3222, 1626, 1582, 1492, 1454, 1253, 1199, 1114, 900, 751 cm^{-1}. ^1H NMR ($CDCl_3$) δ (ppm): 3.49 (s, 4H), 6.56 (d, 4H, $J = 9$ Hz), 6.75 (d, 4H, $J = 9$ Hz), 6.79–7.01 (m, 12H). ^{13}C NMR ($CDCl_3$) δ (ppm): 116.0, 118.7, 119.6, 120.0, 120.3, 123.0, 123.8, 123.8, 142.2, 147.0, 147.4, 148.9, 149.0.

2.4. Polymer Preparation. *BPDA-M1*. High molecular weight poly(amic acid)s were prepared from equimolar dianhydride and diamine monomers in NMP (15% solids) at room temperature. A typical polymerization was carried out as follows: A 100 mL two-neck flask equipped with overhead stirrer and nitrogen inlet was charged with 1.754 g (0.006 mol) of 1,3-bis(4-aminophenoxy)benzene (***M*1**) and 10 mL of dry NMP. This suspension was stirred for 20 min at room temperature to allow the diamine monomer to dissolve. 3,3′,4,4′-Biphenyltetracarboxylic dianhydride (BPDA), 1.765 g (0.006 mol), was dissolved in 10 mL of dry NMP and added to the diamine solution under a stream of dry nitrogen. Polymerization was allowed to proceed for 24 h under a nitrogen atmosphere. The obtained poly(amic acid) had a inherent viscosity of 0.86 g/dL.

Film Preparation. The poly(amic acid)s were centrifuged for 2 h in order to remove suspended solids and cast onto clean glass plates (film thickness ~ 0.43 mm). The obtained films were dried for 2 days in an air-purged low-humidity chamber. Tack-free films were thermally imidized using a conventional hot air convection oven. Imidization was achieved after the films were exposed successively to 100 °C for 1 h, 200 °C for 1 h, and 300 °C for 1 h.

3. Results and Discussion

Monomer Synthesis. The all *para* aryl ether-based diamines, i.e., bis[4-(4-aminophenoxy)phenyl] ether (***P*2**) and 1,4-bis[4-(4-aminophenoxy)phenoxy]benzene (***P*3**), were synthesized as shown in Scheme 1.

Bis[4-(4-aminophenoxy)phenyl] ether (***P*2**) was prepared using conventional fluorine displacement chemistry followed by the catalytic reduction of the obtained dinitro intermediate to the desired diamine monomer. The synthesis of 1,4-bis[4-(4-aminophenoxy)phenoxy]benzene (***P*3**), on the other hand, required a multistep approach. The key intermediate, 1,4-bis(4-hydroxyphenoxy)benzene (**5**), was synthesized using a method reported by Yeager et al.[7] The condensation of hydroquinone (**3**) in the presence of fluorobenzaldehyde yielded the corresponding 4-aryloxydialdehyde (**4**), and a Baeyer–Villiger oxidation of (**4**) in the presence of 3-chloroperoxybenzoic acid (*m*-CPBA) gave the corresponding 4-aryloxy bisformate, which was immediately hydrolyzed to the desired 1,4-bis(4-hydroxyphenoxy)benzene (**5**).

The synthetic approach toward bis[3-(4-aminophenoxy)phenyl] ether (***M*2**) and 1,3-bis[3-(4-aminophenoxy)phenoxy]benzene (***M*3**) is summarized in Scheme 2.

Scheme 2. Synthesis of Bis[3-(4-aminophenoxy)phenyl] Ether (*M*2) and 1,3-Bis[3-(4-aminophenoxy)phenoxy]benzene (*M*3)

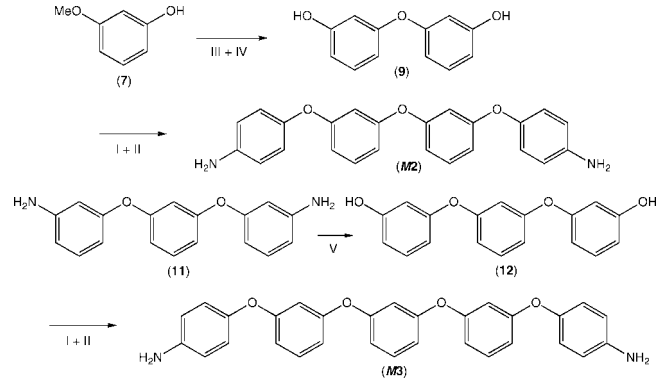

I: DMAc/K_2CO_3 and 1-fluoro-4-nitrobenzene, reflux for 12 h.
II: THF and 10% Pd-C/H_2, room temperature for 4 h.
III: Toluene/NaOMe and 3-bromoanisole/pyridine/CuCl, reflux for 12 h.
IV: HOAc and 48% HBr, reflux for 12 h.
V: 35% H_2SO_4 and $NaNO_2$ at 0 °C and boiling H_2O/H_2SO_4

Both compounds were synthesized in a similar fashion as discussed for the *para*-catenated diamines and started with the synthesis of the required *meta*-substituted bisphenols, i.e., 3,3′-oxydiphenol (**9**) and 1,3-bis(3-hydroxyphenoxy)benzene (**12**). The condensation of 3-methoxyphenol (**7**) with 3-bromoanisole under classic Ullmann conditions gave the bis(3-methoxyphenyl) ether, which after demethylation yielded 3,3′-oxydiphenol (**9**).[8] 1,3-Bis(3-hydroxyphenoxy)benzene (**12**) was conveniently prepared from commercially available 1,3-bis(3-aminophenoxy)-benzene by following a standard Sandmeyer procedure.[12] Both diamine monomers, ***M*2** and ***M*3**, are believed to be new compounds.

The *ortho*-catenated diamines could be synthesized readily, however, overall yields were low mainly because the yields of the intermediate *ortho*-catenated bisphenols were low (~20%). Once 2,2′-oxydiphenol (**18**) and 1,2-bis(2-hydroxyphenoxy)-benzene (**21**) were synthesized, the fluorine displacement reaction proceeded smoothly. The synthesis of 1,2-bis(4-aminophenoxy)benzene (***O*1**), bis[2-(4-aminophenoxy)phenyl] ether (***O*2**), and 1,2-bis[2-(4-aminophenoxy)phenyl] ether (***O*3**) is summarized in Scheme 3. Both diamine monomers, ***O*2** and ***O*3**, are believed to be new compounds.

Synthesis of the Poly(ether imide)s. Polymerization of the all *para*-substituted aryl ether diamines, i.e., ***P*1**, ***P*2**, and ***P*3**, with BPDA or ODPA proceeded smoothly and highly viscous poly(amic acid) solutions, with inherent viscosities ranging from 0.7 to 1.7 dL/g, were obtained. After thermal imidization, tough and flexible pale yellow films were obtained, which could be handled without difficulty. The fully imidized films were not soluble in CH_2Cl_2, DMAc or *m*-cresol at 25 °C ($C = 10$ mg polymer/mL).

The *meta*-substituted arylether diamines, i.e., ***M*1**, ***M*2**, and ***M*3**, could be polymerized without difficulty as well. Inherent viscosities ranged from 0.6 to 1.8 dL/g, and after the thermal imidization tough and flexible yellow films were obtained. The fully imidized ODPA-M2 was soluble in DMAc and *m*-cresol at 25 °C, while the ODPA-M3 film appeared soluble in CH_2Cl_2, DMAc, and *m*-cresol at 25 °C. Good quality films could be cast from CH_2Cl_2 and DMAc (10 wt % solutions).

Polymerization of the *ortho*-substituted aryl ether diamines appeared more challenging. Both BPDA and ODPA could be polymerized with the ***O*1** diamine without difficulty. The inherent viscosity of the corresponding poly(amic acid)s was 1.6 and 0.8 dL/g, respectively, and tough and flexible films were obtained after thermal imidization. The polymerization of BPDA and ODPA with the ***O*2** diamine, on the other hand, resulted in gel-like poly(amic acid)s, which in both cases could not be

Scheme 3. Synthesis of 1,2-Bis(4-aminophenoxy)benzene (*O*1), Bis[2-(4-aminophenoxy)phenyl] Ether (*O*2), and 1,2-Bis[2-(4-aminophenoxy)phenyl] Ether (*O*3)

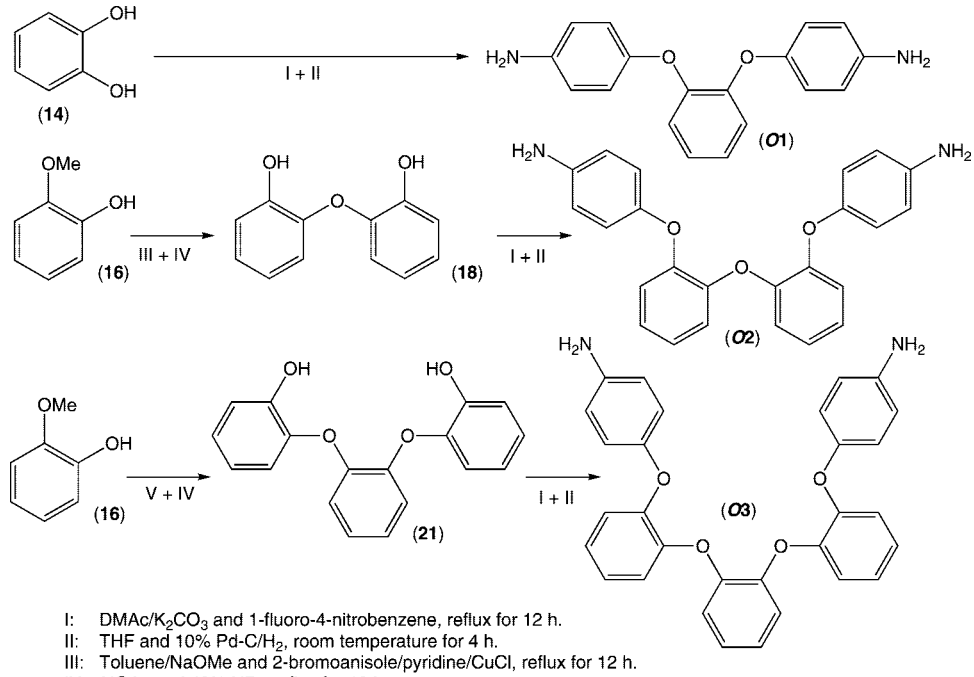

I: DMAc/K_2CO_3 and 1-fluoro-4-nitrobenzene, reflux for 12 h.
II: THF and 10% Pd-C/H_2, room temperature for 4 h.
III: Toluene/NaOMe and 2-bromoanisole/pyridine/CuCl, reflux for 12 h.
IV: HOAc and 48% HBr, reflux for 12 h.
V: CH_3CN/K_2CO_3 and 1,2-dibromobenzene, reflux for 12 h.

Table 1. Inherent Viscosities of Poly(amic acid)s and the Quality of Their Corresponding Poly(ether imide) Films

polymer	η_{inh}[a] (dL/g)	film quality[b]	polymer	η_{inh}[a] (dL/g)	film quality[b]	polymer	η_{inh}[a] (dL/g)	film quality[b]
BPDA-***P*1**	1.67	flexible	BPDA-***M*1**	0.86	flexible	BPDA-***O*1**	1.60	flexible
BPDA-***P*2**	1.01	flexible	BPDA-***M*2**	1.80	flexible	BPDA-***O*2**	1.03	brittle
BPDA-***P*3**	0.77	flexible	BPDA-***M*3**	1.44	flexible	BPDA-***O*3**	0.50	flexible
ODPA-***P*1**	0.72	flexible	ODPA-***M*1**	0.92	flexible	ODPA-***O*1**	0.75	flexible
ODPA-***P*2**	1.18	flexible	ODPA-***M*2**	0.73	flexible	ODPA-***O*2**	1.08	brittle
ODPA-***P*3**	0.87	flexible	ODPA-***M*3**	0.59	flexible	ODPA-***O*3**	0.26	flexible

[a] Viscosities of the poly(amic acid)s were measured at a concentration of 0.5 g/dL in NMP at 25 °C using an Ubbelohde, viscometer (100/B 825). [b] Films were cast by slow evaporation of the polyamic acid NMP solution followed by a thermal imidization protocol.

stirred. Both solutions were diluted from 15% solids to 10% solids and heated to 70 °C in order to cast useful amic acid films. Although both poly(amic acid)s exhibited inherent viscosities of 1.0 and 1.1 dL/g, respectively, the fully imidized BPDA-***O*2** and ODPA-***O*2** films appeared highly crystalline and very brittle in nature. The films could not be handled. The polymerization of BPDA and ODPA with the ***O*3** diamine resulted in low inherent viscosity poly(amic acid)s, which is thought to be due to the formation of cyclic species.[13,14] Despite the low inherent viscosities of 0.5 and 0.3 dL/g, respectively, the imidized films are tough, flexible, and easy to handle. None of the ***O*1**-, ***O*2**-, or ***O*3**-based polymers appeared soluble in CH_2Cl_2, DMAc, or *m*-cresol at 25 °C. The inherent viscosities of all poly(amic acid)s are summarized in Table 1.

Dynamic Thermogravimetric Analysis. The thermal stability of the poly(ether imide)s were evaluated using polymer films which were dried under vacuum at 150 °C for 24 h. The decomposition temperatures, the temperature at which 5% weight loss occurred using a heating rate of 2.5 °C/min, and the char yields for the polymers are listed in Table 2. Samples were investigated under oxidative (air) and inert (nitrogen) conditions.

In general, it can be stated that all polymers show excellent thermal stabilities in both air and nitrogen environments, and the observed $T_{5\%}$ values are typical for all-aromatic poly(ether imide)s. Although it is difficult to recognize trends, it certainly appears that the polymers based on the *meta*-aryl ether diamines exhibit somewhat better thermal stabilities under both oxidative and inert conditions; i.e., the $T_{5\%}$ values are on average ~10–20 °C higher as compared to the *para*- and *ortho*-based analogues. The data in Table 2 also indicate that increasing the number of *para*-, *meta*-, or *ortho*-aryl ether units (X in Figure 1 = 1, 2, or 3) decreases the thermal stability under both inert and oxidative conditions. The difference in thermal stability between BPDA- and ODPA-based polymers appears minimal. The char yields of the *para*- and *meta*-based polymers, heated under a nitrogen

Table 2. Thermal and Thermooxidative Properties of the Poly(ether imide) Films

	TGA 5% weight loss (°C)		char yield (%) at 600 °C	
polymer	air	N_2	air	N_2
BPDA-***P*1**	488	524	1	71
BPDA-***P*2**	479	514	1	68
BPDA-***P*3**	454	496	2	67
ODPA-***P*1**	482	499	0	64
ODPA-***P*2**	477	506	1	62
ODPA-***P*3**	461	481	2	57
BPDA-***M*1**	493	533	2	74
BPDA-***M*2**	461	502	1	73
BPDA-***M*3**	490	514	1	71
ODPA-***M*1**	464	503	1	67
ODPA-***M*2**	499	502	3	66
ODPA-***M*3**	480	501	0	66
BPDA-***O*1**	494	539	3	85
BPDA-***O*2**	445	499	3	62
BPDA-***O*3**	448	480	9	58
ODPA-***O*1**	478	490	6	63
ODPA-***O*2**	459	509	1	59
ODPA-***O*3**	434	480	0	53

Table 3. Thermal and Mechanical Properties of the Poly(ether imide)s[a]

polymer	morphology[b]	T_g (°C) DSC[c]	T_m (°C) DSC[d]	T_g (°C) DMTA	E' (GPa) 30 °C	T_g (°C) calcd	ΔT_g (°C) DSC
BPDA-***P*1**	SC	272	457	301	2.4	257	−15
BPDA-***P*2**	SC	226	381	253	2.2	229	+3
BPDA-**P3**	SC	218	345	231	2.5	209	−9
ODPA-***P*1**	Am	243		258	2.7	243	0
ODPA-***P*2**	Am	214		227	2.6	219	+5
ODPA-***P*3**	Am	206		205	2.5	201	−5
BPDA-***M*1**	SC	214	384	259	3.0	217	+3
BPDA-***M*2**	Am	196		197	2.0	188	−8
BPDA-***M*3**	Am	173		176	2.6	168	−5
ODPA-***M*1**	Am	215		226	2.8	211	−4
ODPA-***M*2**	Am	175		191	1.9	185	+10
ODPA-***M*3**	Am	158		166	2.6	167	+9
BPDA-***O*1**	Am	246		251	2.6	224	−22
BPDA-***O*2**	SC	206			−[e]	193	−13
BPDA-***O*3**	Am	184		208	2.5	171	−13
ODPA-***O*1**	Am	223		227	2.5	219	−4
ODPA-***O*2**	SC	190			−[e]	192	2
ODPA-***O*3**	Am	171			—[f]	171	0

[a] DSC (second heating) and DMTA data were collected using a heating rate of 10 and 2.5 °C/min, respectively. [b] Morphology: SC = semicrystalline; Am = amorphous (after second heat). [c] T_g is reported at the inflection point. [d] T_m is reported as the peak temperature. [e] Sample too brittle to handle. [f] Not enough material vailable for DMTA analysis.

atmosphere, are in the range of ∼65–70%. The *ortho*-based polymers are different in that both BPDA-***O*1** and ODPA-***O*1** polymers exhibit the highest observed char yields, i.e., 85% and 81%, respectively. The ***O*2**- and ***O*3**-based polymer, on the other hand, exhibit the lowest observed char yields and are in the range 53–59%. It is, however, impossible to draw any hard conclusions from these results since the thermal stability of polymers depends on a variety of factors, including the molecular weight, molecular weight distribution, and the presence of species that catalyze the thermal degradation of polymers.

Differential Scanning Calorimetry. The phase behavior of our polymers was investigated using differential scanning calorimetry. Samples were heated at 10 °C/min under a nitrogen atmosphere to 400 °C. The DSC results of the second heating scans are summarized in Table 3.

The ODPA and BPDA series based on the all *meta*-substituted aryl ether diamines; i.e., ***M*1**, ***M*2**, and ***M*3** series gave amorphous films with the exception of BPDA-***M*1**. This semicrystalline film shows a melt endotherm at 384 °C and a crystallization exotherm on cooling. The observed phase behavior agrees with what has been reported by Wilkes et al.[15] Attempts to quench the film in the amorphous state were not successful. Introducing *meta*-substituted aryl ether spacers is a very efficient method to lower the T_g and improve the processability. The large increase in free volume associated with *meta*-linked aryl ethers, however, appears to disrupt the delicate intermolecular interactions that promote mesophase behavior in this class of rigid polymers. None of the polymers based on our *meta*-based diamines form a liquid crystalline phase.

When the BPDA and ODPA dianhydrides were polymerized with the all *para*-substituted aryl ethers, the ODPA series resulted in amorphous films. The BPDA series, on the other hand, i.e., BPDA-***P*1**, -***P*2**, and -***P*3**, gave semicrystalline films. The polymers showed reversible melting and crystallization upon heating and cooling, and a DSC trace of BPDA-***P*3**, second heating after quenching, is shown in Figure 2.

Similar DSC thermograms were obtained upon successive heating and cooling experiments, confirming the thermoplastic nature of the all-aromatic poly(ether imide). The crystallization kinetics of this series is currently under investigation. Finally, the ODPA and BPDA series based on the all *ortho*-substituted aryl ether diamines; i.e., the ***O*1**, ***O*2**, and ***O*3** series gave amorphous films. Both BPDA-***O*2** and ODPA-***O*2**, however, showed a melting endotherm at 318 and 316 °C, respectively,

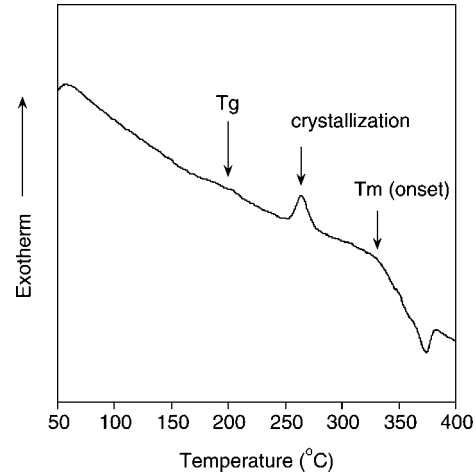

Figure 2. DSC trace of our BPDA-***P*3** poly(ether imide) showing the thermoplastic nature of this polymer. Second heat, measured at a heating rate of 10 °C/min.

on the first heat. The second heating did not reveal a melt transition but a T_g only, suggesting that the melting endotherm was solvent (NMP) induced.

The T_g's for polymers from both dianhydrides, i.e., BPDA and ODPA, are plotted as a function of the number and type of aryl ether spacer in Figure 3. The largest drop in T_g is observed for the *meta*-substituted aryl ethers, whereas *para*- and *ortho*-substitution appears to have a comparable effect on lowering the T_g. Increasing the number of aryl ether units (X) to, for example 4 or 5, does not appear to lower the T_g much further.

Dynamic Mechanical Thermal Analysis. The mechanical properties of the poly(ether imide)s were examined in the temperature range 25−500 °C at 1 Hz. All films were dried under vacuum at 125 °C prior to use. The DMTA results, i.e., the T_g as determined at the maximum of tan δ and the storage modulus (E'), are summarized in Table 3. All poly(ether imide) films show storage moduli (E') of 2–3 GPa, which is typical for this class of polymers. The T_g values, as determined by DMTA, confirm the same trend as observed by DSC; i.e., when the number of aryl ether units in the polymer backbone increase, the T_g goes down. An interesting observation is the fact that both the BPDA and ODPA series based on ***P*1**, ***P*2**, or ***P*3** diamines all show β-transitions with a maximum around 90 °C. Polymers based on *meta*- or *ortho*-substituted aryl ether diamines

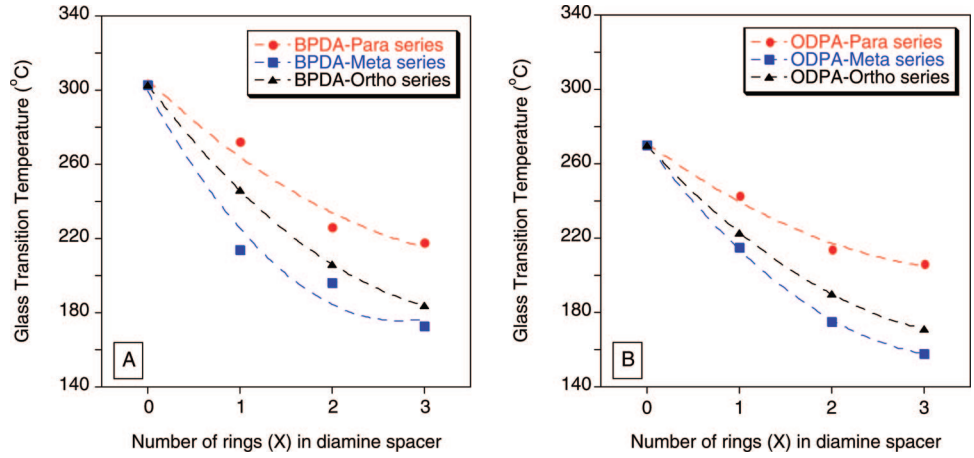

Figure 3. T_g as a function of the substitution pattern and number of aryl ether units (X) in (A) the BPDA polymer series and (B) the ODPA polymer series. The T_g values for $X = 0$ are included for reference purposes.[16]

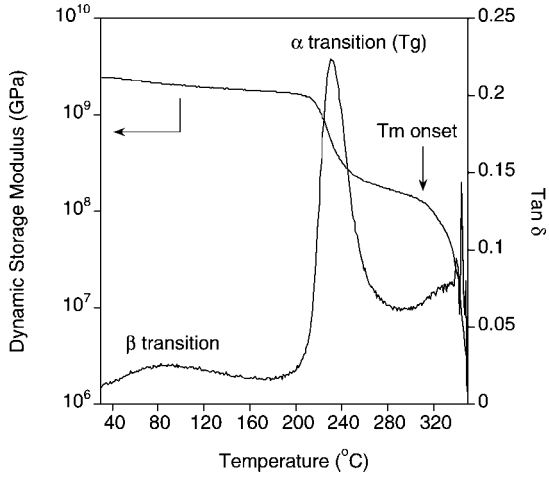

Figure 4. Storage modulus (E') of BPDA-***P3*** as measured by DMTA. The experiment was conducted at a frequency of 1 Hz, while heating at 2.5 °C/min.

show no sign of sub-T_g transitions. The DMTA thermogram of BPDA-***P3*** is shown in Figure 4.

The thermogram is typical of a semicrystalline thermoplastic polymer. Once the polymer has passed through the T_g, the modulus drops somewhat but reaches a rubber plateau, followed by the melting of the crystalline regions beginning at 320 °C.

Polarizing Optical Microscopy. We used hot-stage optical microscopy to study the melt behavior of the poly(ether imide) films and by doing so gain insight into the phase type and phase stability as a function of the temperature. All films were investigated under ambient conditions and heated to 500 °C using a heating and cooling rate of 20 °C/min. From the 18 synthesized poly(ether imide) films only one polymer, i.e., BPDA-***P3***, melts into a liquid crystal phase.[17] BPDA-***P3*** forms upon heating a classic nematic Schlieren texture, which is indicative of a mesophase where the molecules show long-range order but lack positional order.[18] Although the polymer starts to melt around 350 °C, the viscosity is initially too high for a liquid crystal texture to develop. At 400 °C, as can be seen in Figure 5a, a nematic texture could be clearly observed.

We were not able to detect a nematic to isotropic (N−I) transition below 500 °C, at which point the polymer started to show signs of thermal oxidative degradation. Successive heating and cooling experiments confirmed the enantiotropic phase behavior of this polymer. Although most imide-based liquid crystal polymers reported to date have a strong tendency to develop smectic phases,[3] thought to be due to strong intermolecular imide−imide interactions, we were not able to detect higher order phases.

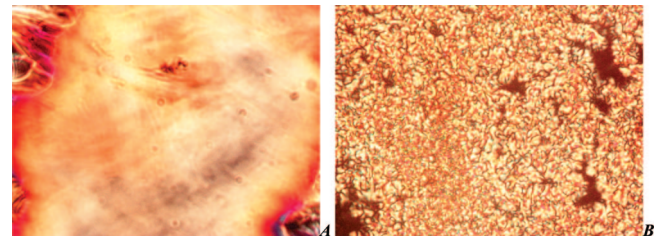

Figure 5. (A) Microphotograph of BPDA-***P3*** between crossed polarizers (20×); high viscous nematic texture at 400 °C. (B) BPDA-***P3*** (5000 g mol^{-1}, phthalic anhydride end-capped); low viscous nematic Schlieren texture at 250 °C; between crossed polarizers (20×).

The fact that BPDA-***P3*** is able to melt into a liquid crystalline phase can be understood as follows. When one considers the "parent" compound, i.e., BPDA-***P1***, $X = 1$ in the figure below, it is clear that this molecule meets the definition of a classic rigid rod polymer. This polymer, however, does not exhibit liquid crystallinity because $T_m \gg T_d$. The next member of this homologues series, where $X = 2$, does melt, but adding an extra *para*-aryl ether unit disrupts the linear progression of the polymer backbone and results in an isotropic melt. Adding one more *para*-aryl ether unit ($X = 3$; BPDA-***P3***) restores the backbone linearity and a stable liquid crystalline melt becomes accessible.

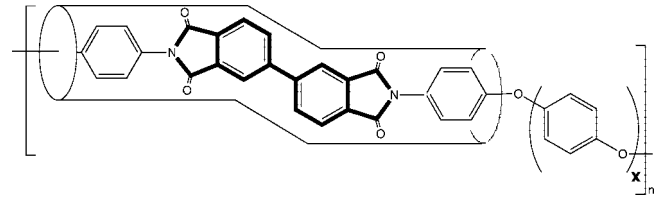

In order to obtain more discernible liquid crystalline textures, we synthesized a series of low molecular weight oligomers by using phthalic anhydride to end-cap the polymer chain and limit the M_n to 5000 g mol^{-1}. This approach resulted in inert oligomers with lower melting points and lower melt viscosities; the latter is expected to result in improved texture formation. In addition to using BPDA, we also used PMDA and NDA as mesogenic diimide cores as summarized in Figure 6.

Although the NDA- and PMDA-based oligomers have molecular features conducive to liquid crystal formation their

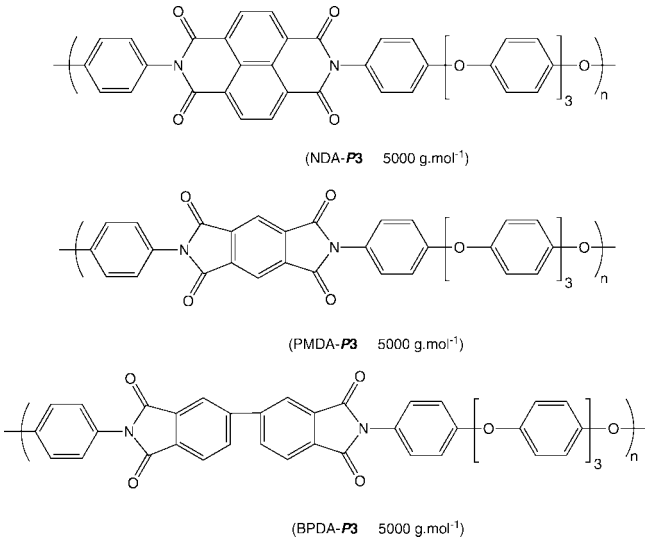

Figure 6. PEI oligomers based on mesogenic dianhydrides, i.e., 1,4,5,8-tetracarboxylic dianhydride (NDA), pyromellitic dianhydride (PMDA), and 3,3′,4,4′-biphenyltetracarboxylic dianhydride (BPDA), reacted with ***P3*** diamine. All oligomers have an $M_n \sim 5000$ g mol^{-1} and were end-capped with phthalic anhydride.

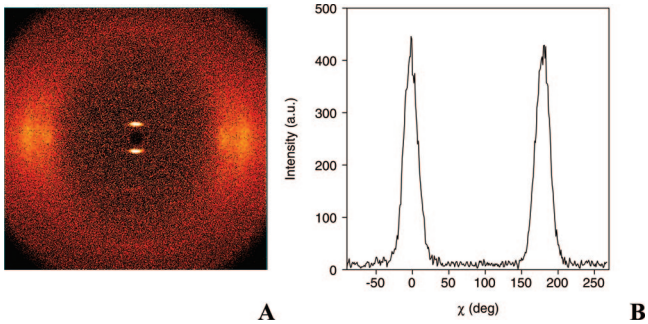

Figure 7. (A) X-ray diffraction pattern and (B) intensity plot of the low angle diffraction peaks of an aligned BPDA-***P3*** film measured at 24 °C. The film was aligned by stretching the film (by 200%) in the nematic phase at 370 °C. Draw direction: vertical.

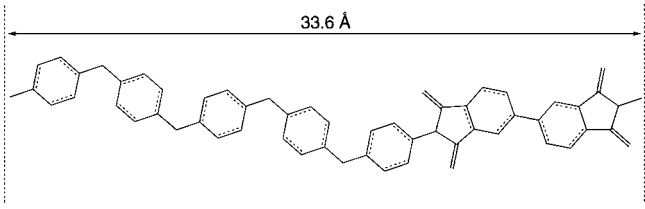

Figure 8. All-trans configuration of BPDA-***P3*** as calculated by MM2.

rigid character prevents the formation of an accessible melt transition. Both oligomers were investigated using fast heating rates of 50 °C min^{-1} in order to prevent side reactions such as cross-linking or thermal decomposition, but we were not able to detect a melt transition up to 450 °C. The rotational freedom available in BPDA biphenyl core seems to be a prerequisite toward LC formation in this class of polymers. The 5000 g mol^{-1} BPDA-***P3*** oligomer melts at 250 °C and exhibits a lower melt viscosity, as expected. The liquid crystal window is significantly compromised due to a lower aspect ratio and only persists over a 30 °C window, after which the sample melts into the isotropic phase. A microphotograph of the nematic Schlieren texture at 250 °C is shown in Figure 5b.

X-ray Diffraction Analysis. In addition to the POM observations, we used XRD analysis to confirm the liquid crystalline nature of BPDA-***P3***. We prepared an aligned sample by stretching a piece of BPDA-***P3*** film in the nematic phase, i.e., at 370 °C, followed by immediately quenching the sample to room temperature. This film was then used for XRD analysis. Figure 7a shows the diffraction pattern as recorded at room temperature. The XRD experiment revealed a typical scattering pattern, characteristic for an aligned liquid crystalline polymer.

The diffraction pattern of BPDA-***P3*** shows scattering from both the lateral intermolecular spacing between adjacent polymer chains (~4.8 Å; on the equator) and the repeat distance normal to the strata (33.2 Å; meridional scattering). This diffraction pattern is indicative for a smectic A (SmA) supramolecular structure and agrees with the length of the polymer repeat unit, i.e., 33.6 Å in the *all-trans* configurations as calculated by MM2 (shown in Figure 8).

Scattering data on the 2-D detector was integrated on the 2θ direction over a ring containing the scattering peaks, resulting in a scattering intensity as a function of the azimuthal angle, χ (Figure 7B). A bimodal Maier−Saupe function, eq 1, was used to fit the obtained curve in order to extract the two peak positions, χ_1 and χ_2 and widths, α_1 and α_2.[19] In this expression, i_0 is an arbitrary baseline.

$$i(\chi) = i_0 + A_1 \exp(\alpha_1 \cos^2(\chi - \chi_1)) + A_2 \exp(\alpha_2 \cos^2(\chi - \chi_2)) \quad (1)$$

From the peak width α values, obtained from the fitting of the peaks of Figure 7B with eq 1, one can easily calculate the value for the experimental order parameter, S_{exp}, which can be defined in the present case as a product of two contributions:[20]

$$S_{exp} = \langle P_2 \rangle \overline{P_2} = \overline{\langle P_2 \rangle} \quad (2)$$

where $\langle P_2 \rangle$ is the local molecular order parameter. $\overline{P_2}$ is the macroscopic director order parameter. From the α parameter, the average orientational order parameter $\overline{\langle P_2 \rangle}$ is determined using

$$\overline{\langle P_2 \rangle} = \frac{\int_{-1}^{1} P_2(\cos\beta) e^{\alpha \cos^2\beta} \, d\cos\beta}{\int_{-1}^{1} e^{\alpha \cos^2\beta} \, d\cos\beta} \quad (3)$$

where $P_2(\cos\beta)$ is the second-order Legendre polynomial of $\cos(\beta)$:

$$P_2(\cos\varphi) = \frac{1}{2}(3\cos^2\varphi - 1) \rightarrow P_2(\cos\beta) = \frac{1}{2}(3\cos^2\beta - 1) \quad (4)$$

This procedure, described in detail elsewhere,[19] reveals an order parameter, $\langle P_2 \rangle$, of 0.87, an order parameter typical for highly aligned liquid crystalline polymers. Although BPDA-***P3*** was aligned and quenched from the nematic phase, the resulting polymer film shows a high degree of smectic ordering. The current experiments are not able to differentiate quantitatively between SmA and nematic ordering.

In comparison, we also determined the order parameter of an aligned ODPA-***P3*** film (polymer was aligned by stretching a film sample by 200% at 350 °C). This polymer is almost identical to BPDA-***P3***, with the exception that it contains a flexible oxygen linkage in the ODPA dianhydride moiety. The latter will reduce the rigidity and hence the mesogenicity of the polymer backbone. ODPA-***P3*** forms an isotropic melt, as determined by hot stage optical microscopy, and exhibits an order parameter $\langle P_2 \rangle = 0.24$. This polymer does not show low angle reflections; hence, the order parameter was determined using the broad reflections at $2\theta \sim 18°$.

Quantitative Structure–Property Relationships. There have been many attempts to quantify the relationship between polymer structure and glass transition temperature (T_g). Some schemes such

as those of Van Krevelen[21] and Bicerano[22] make no prior assumptions about the physical factors that influence T_g. Others begin with intuitive generalizations about the effects of chain stiffness, side groups, intermolecular forces, and symmetry of substitution.[23] Herein we expand on the latter approach.

Following Hayes,[24] T_g should be related to numbers of rotational degrees of freedom and to cohesive energies. In the case of our all-aromatic chains, it is easy to count the number of rotatable bonds that change the chain trajectory. We then normalized this number of bonds per repeat unit by the mass of the repeat unit to give a flexibility parameter. If this normalization is not included, T_g appears to depend strongly on the mass of the repeat unit[25,26] —an unphysical result, since the definition of the repeating unit in a high polymer is somewhat arbitrary and the smallest identifiable repeat units of our polymers vary widely in size. "Chain stiffness" is then the inverse of the flexibility parameter.

Intermolecular energetics are reflected in such quantities as cohesive energy.[24] We seek a *molecular* descriptor related to the intermolecular attraction. For small molecules, hundreds of descriptors have been proposed.[27] We have chosen to use the total of the (squared) atomic charges (again per mass). The intent is to describe, in the simplest possible way, the interactions in a given volume of material. We are using mass in place of volume because densities of amorphous poly(ether imide)s do not vary greatly; furthermore, simulation of the molecular packing is a much more difficult process and hardly justified at this level of approximation. Atomic charges were assigned using AM1 semiempirical quantum calculations (Hyperchem) on suitably end-capped substructures.

Having chosen flexibility and attractive parameters, it remains to determine the appropriate fitting function to relate them to T_g. A generalized dependence on the two descriptors (e.g., Boyer[28]) could be summarized by various techniques, including perhaps neural networks, but simple linear regression was found to be adequate for our purposes. The regression coefficients were determined by fitting to literature values of T_g for 20 homo- and copolyimides containing only ether hinges.[29–33] The resulting equation is

$$T_g = -195.36 + 0.70a_1 + 103936a_2 \quad (5)$$

where a_1 is the mass per rotatable bond and a_2 is the squared charge (in electron charges) per molecular mass (in amu). The calculated T_g values in Table 3 show good agreement (±10 °C) with the T_g data obtained from our DSC experiments.

4. Conclusions and Concluding Remarks

We have synthesized a systematic series of nine all-aromatic diamines built around *para*-, *meta*-, and *ortho*-substituted aryl ether units, with either 2, 3, or 4 ether units per monomer. These "flexible" diamines were polymerized with 3,3′,4,4′-biphenyl dianhydride (BPDA) and 3,3′,4,4′-oxydiphthalic dianhydride (ODPA) in order to investigate the possibility of forming all-aromatic poly(ether imide)s with liquid crystal properties. The general observation is that the thermal transition temperatures, T_g and T_m, drop rapidly when the number of aryl ether units increase (*para* > *ortho* > *meta*) but seem to level off at 3, indicating that an additional aryl ether unit will not lower the T_g and/or T_m much further. As determined by DSC, TGA, and DMTA, all polymers show excellent thermal (T_g's ~158–272 °C) and mechanical properties (E' ~ 2–3 GPa). With the exception of BPDA-***M*1** and the BPDA-$\boldsymbol{P_X}$ series, we observed that all polymers form amorphous polymer films and when 3 or 4 flexible ether linkages were introduced these polymers become thermoplastic in nature. From the 18 polymers we prepared, only one polymer, BPDA-***P*3**, appears mesogenic. This polymer displays a T_g of 218 °C (DSC), and at ~350 °C this polymer melts into a nematic phase. The N−I transition could not be observed since the polymer started to show signs of thermal decomposition at ~500 °C. Highly aligned films could easily be obtained by stretching the films in the nematic phase (370 °C), and after quenching the films, XRD analysis confirmed the presence of a highly aligned (partially) smectic A phase (SmA) with an order parameter $P_2 = 0.9$, indicating a high degree of molecular alignment. To the best of our knowledge, this is the first example of an all-aromatic liquid crystalline poly(ether imide), and we believe that the demonstrated ability to design all-aromatic PEIs with LC properties will prove to be useful in a variety of aerospace and electronics related applications.

Acknowledgment. This research was supported in part by the National Aeronautics and Space Administration under Contract No. NAS1-97046 while T. J. Dingemans was in residence at ICASE, NASA Langley Research Center, Hampton, VA. The authors thank Crystal Topping and Alice Chang for performing the TGA and DSC measurements.

References and Notes

(1) Wilson, D., Stengenberger, H. D., Hergenrother, P. M., Eds. *Polyimides*; Blackie: Glasgow, 1990.
(2) Hergenrother, P. M. *High Perform. Polym.* **2003**, *15*, 3.
(3) (a) Kricheldorf, H. R. *Adv. Polym. Sci.* **1999**, *141*, 83. (b) Tanaka, M.; Konda, M.; Miyamoto, M.; Kimura, Y.; Yamaguchi, A. *High Perform. Polym.* **1998**, *10*, 147. (c) Asanuma, T.; Oikawa, H.; Ookawa, Y.; Yamasita, W.; Matsuo, M.; Yamaguchi, A. *J. Polm. Sci., Part A: Polym. Chem.* **1994**, *32*, 2111.
(4) Dingemans, T. J.; StClair, T. L.; Samulski, E. T. *Chem. Mater.* **2004**, *16*, 966.
(5) The use of trade names of manufacturers does not constitute an official endorsement of such products or manufacturers, either expressed or implied, by the National Aeronautic and Space Administration.
(6) Oesterlin, *Monatsh. Chem.* **1931**, *57*, 31.
(7) Yeager, G. W.; Schissel, D. N. *Synthesis* **1991**, 63.
(8) Sommer, N.; Staab, H. A. *Tetrahedron Lett.* **1966**, 2837.
(9) Eastmond, G. C.; Paprotny, J. *Synthesis* **1998**, 894.
(10) Kime, D. E.; Norymberski, J. K. *J. Chem. Soc., Perkin Trans. 1* **1977**, 1048.
(11) Asfari, Z.; Lamare, V.; Dozol, J.-F.; Vicens, J. *Tetrahedron Lett.* **1999**, *40*, 691.
(12) Sax, K. J.; Saari, W. S.; Mahoney, C. L.; Gordon, J. M. *J. Org. Chem.* **1960**, *25*, 1590.
(13) Adia, S.; Butler, R.; Eastmond, G. C. *Polymer* **2006**, *47*, 2612.
(14) Eastmond, G. C.; Paprotny, J. *Polymer* **2004**, *45*, 1073.
(15) Ratta, V.; Ayambem, A.; McGrath, J. E.; Wilkes, G. L. *Polymer* **2001**, *42*, 6173.
(16) (a) Kochi, M.; Yonezawa, T.; Yokota, R.; Mita, I. *Abstr. Fourth Int. Conf. Polyimides* **1991**, 13–20. (b) Harris, F.; Seymour, R. *Structure-Solubility Relationships in Polymers*; Academic Press: Amsterdam, 1977; p 204.
(17) Dingemans, T. J.; Weiser, E. S.; Hinkley, J. A.; StClair, T. L. US Patent Application LAR-17402-1, 2007.
(18) Collings, P. J.; Hird, M. *Introduction to Liquid Crystals*; Taylor and Francis: New York, 1997; Chapter 1.
(19) Picken, S. J.; Aerts, J.; Visser, R.; Northolt, M. G. *Macromolecules* **1990**, *23*, 3849.
(20) Zannoni, C. In *The Molecular Physics of Liquid Crystals*; Luckhorst G. R., Gray, G. W., Eds.; Academic Press: New York, 1979; Chapter 3.
(21) Van Krevelen, D. W. *Properties of Polymers*; Elsevier: Amsterdam, 1990.
(22) Bicerano, J. *Prediction of Polymer Properties*; Marcel Dekker: New York, 1996.
(23) Sperling, L. H. *Introduction to Physical Polymer Science*; Wiley: New York, 1992.
(24) Hayes, R. A. *J. Appl. Polym. Sci.* **1961**, *5*, 318.
(25) Hammerton, I.; Howlin, B. J.; Larwood, V. J. *Mol. Graphics* **1995**, *13*, 14.
(26) Collantes, E.; Gahimer, T.; Welsh, W. J.; Grayson, M. *Comput. Theor. Polym. Sci.* **1996**, *6*, 29.
(27) Katritzky, A. R.; Sild, S.; Lobanov, V.; Karelson, M. J. *Chem. Inf. Comput. Sci.* **1998**, *38*, 300.
(28) Boyer, R F. *Macromolecules* **1992**, *25*, 5326.
(29) StClair, T. L.; StClair, A. K.; Smith, E. N. Solubility-Structure Study of Polyimides. In *Structure-Solubility Relationship in Polymers*; Academic Press: New York, 1977.

(30) Srinivas, S.; Caputo, F. E.; Graham, M.; Gardner, S.; Davis, R. M.; McGrath, J. E.; Wilkes, G. C. *Macromolecules* **1997**, *30*, 1012.
(31) Hergenrother, P. M. Heat-Resistant Polymers. In *Encyclopedia of Polymer Science and Engineering*; John Wiley & Sons: New York, 1987.
(32) Jensen, B. J.; Hou, T. H.; Wilkinson, S. P. *High Perform. Polym.* **1995**, *7*, 11.
(33) Bryant, R. G. *High Perform. Polym.* **1996**, *8*, 607.

MA8000324